Additional information

Correspondence and requests for materials should be addressed to R.A.

Reprints and permissions information is available at http://www.nature.com/ reprints.

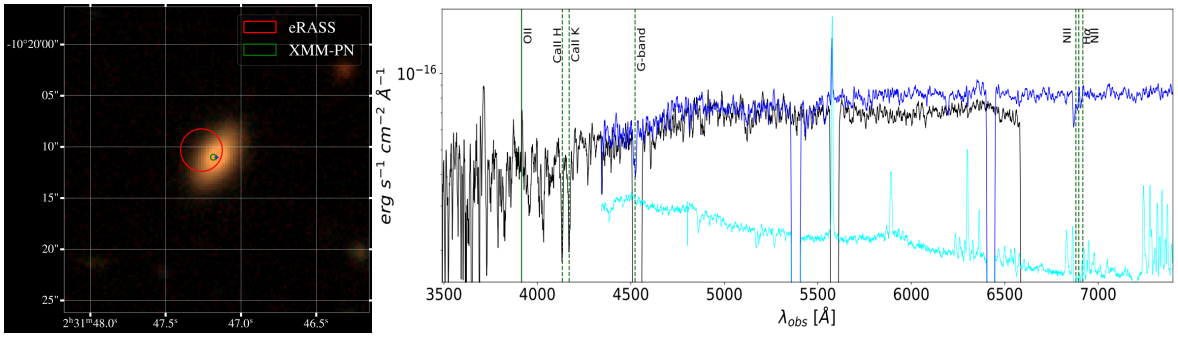

Extended Data Fig. 1 – eRO-QPE1 position and identification. a, Legacy DR8 image cut-out around the optical counterpart of eRO-QPE1. Red and green circles represent the astrometry-corrected eROSITA and XMM-PN positions, respectively, with 1σ positional uncertainties. The EPIC-PN position was corrected excluding the target (blue cross) to ensure an unbiased estimate of the possible positional offset. **b**, SALT spectra of eRO-QPE1 shown in black and blue with related 1σ errors. The cyan spectrum represents a re-normalized sky spectrum to guide the eye for the residual sky feature around 5577Å.

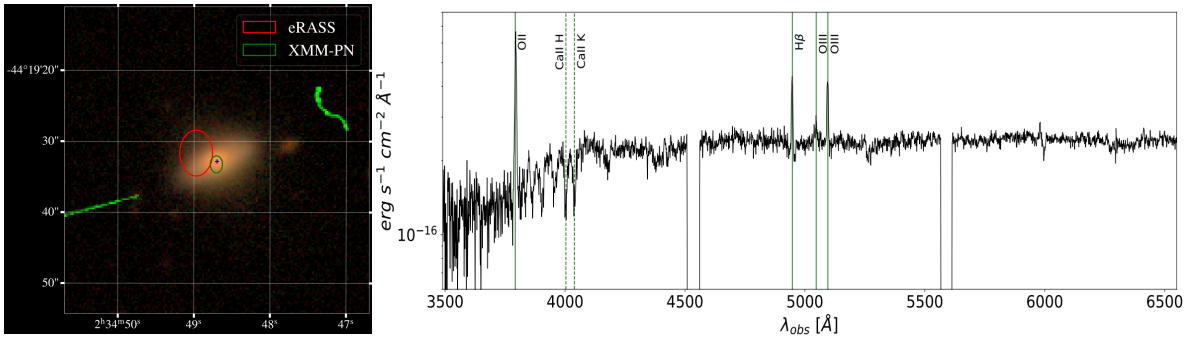

Extended Data Fig. 2 – eRO-QPE2 position and identification. Same as in Extended Data Fig.1, but for eRO-QPE2.

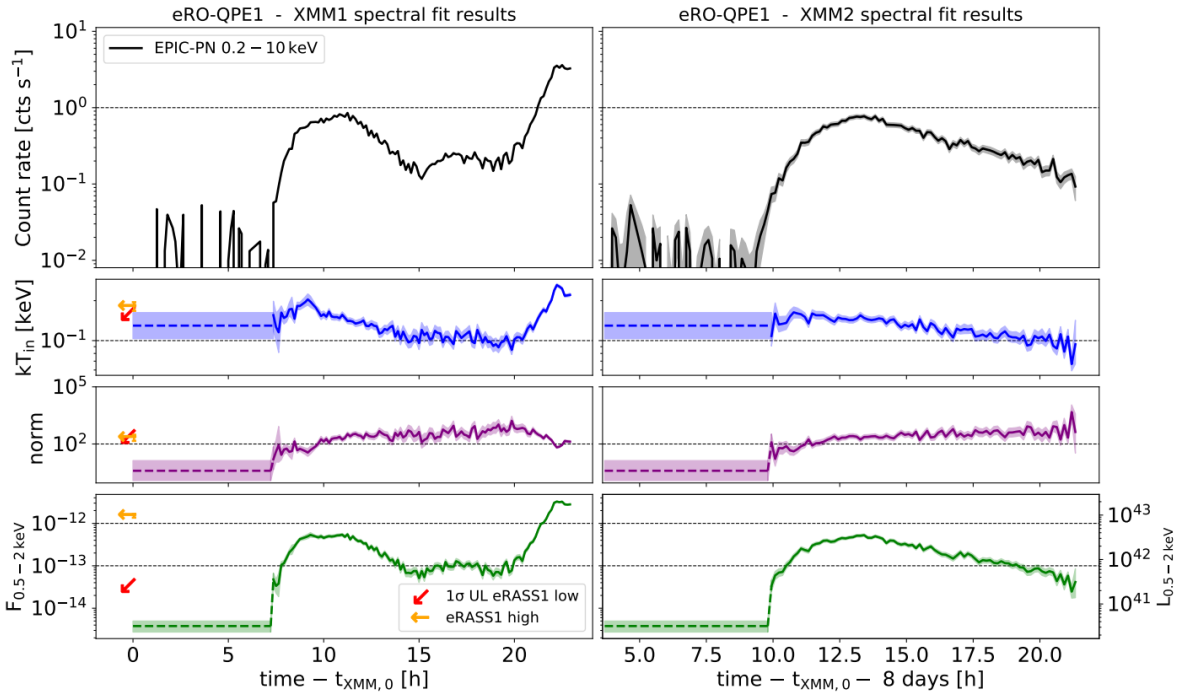

Extended Data Fig. 3 – eRO-QPE1 spectral fit results. PN light-curve (top panel) and time-resolved spectroscopy fit results for spectra extracted in the 500 s time bins (bottom panels) of the two XMM-Newton observations of eRO-QPE1 using an accretion disk model (diskbb): in particular, the evolution of the peak accretion disk temperature and the normalization, which is proportional to the inner radius once distance and inclination are known. The quiescence level is fit combining the first part of both XMM-Newton observations. Median fit values and fluxes of the high and low eROSITA states are reported with orange and red arrows pointing left (upper limits are denoted with diagonal arrows).

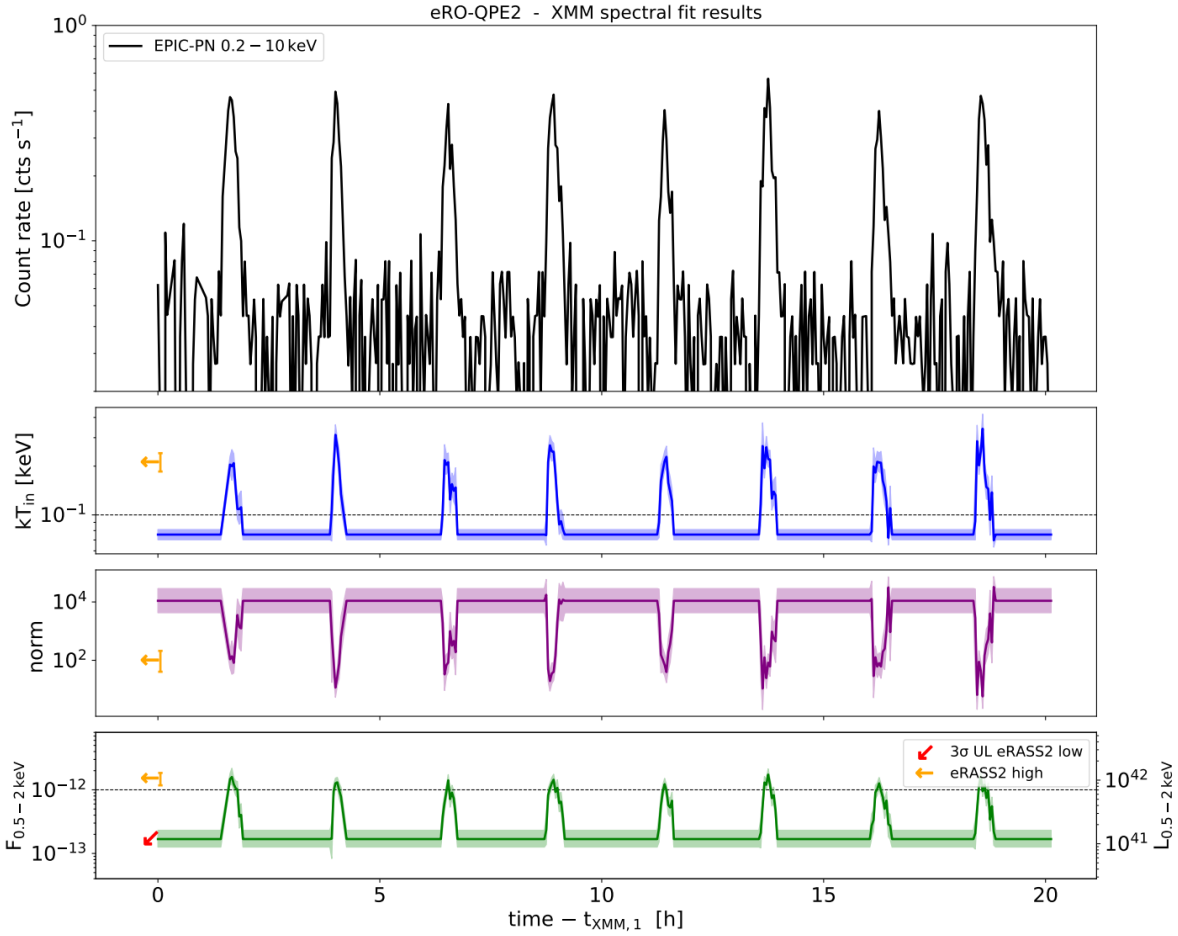

835 **Extended Data Fig. 4 – eRO-QPE2 spectral fit results.** Same as Extended Data Fig. 3, but for
836 eRO-QPE2.

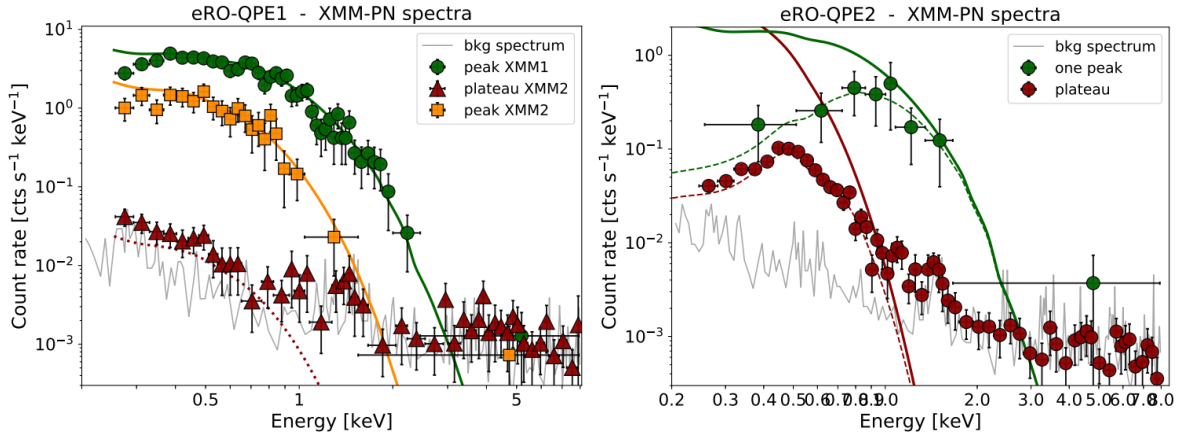

837 **Extended Data Fig. 5 – eRO-QPE1 and eRO-QPE2 spectra. a**, XMM-Newton EPIC-PN source
838 plus background spectra for eRO-QPE1. Red, orange and green data correspond to quiescence and
839 to the peak of the second and first XMM-Newton observation, respectively. The related solid lines
840 show the unabsorbed source model obtained with diskbb, just for visualization. The grey line
841 represents the background spectrum alone. **b**, same as **a** but for eRO-QPE2. Here green data
842 represent one of the peaks and the additional dashed lines indicate the absorbed source model.

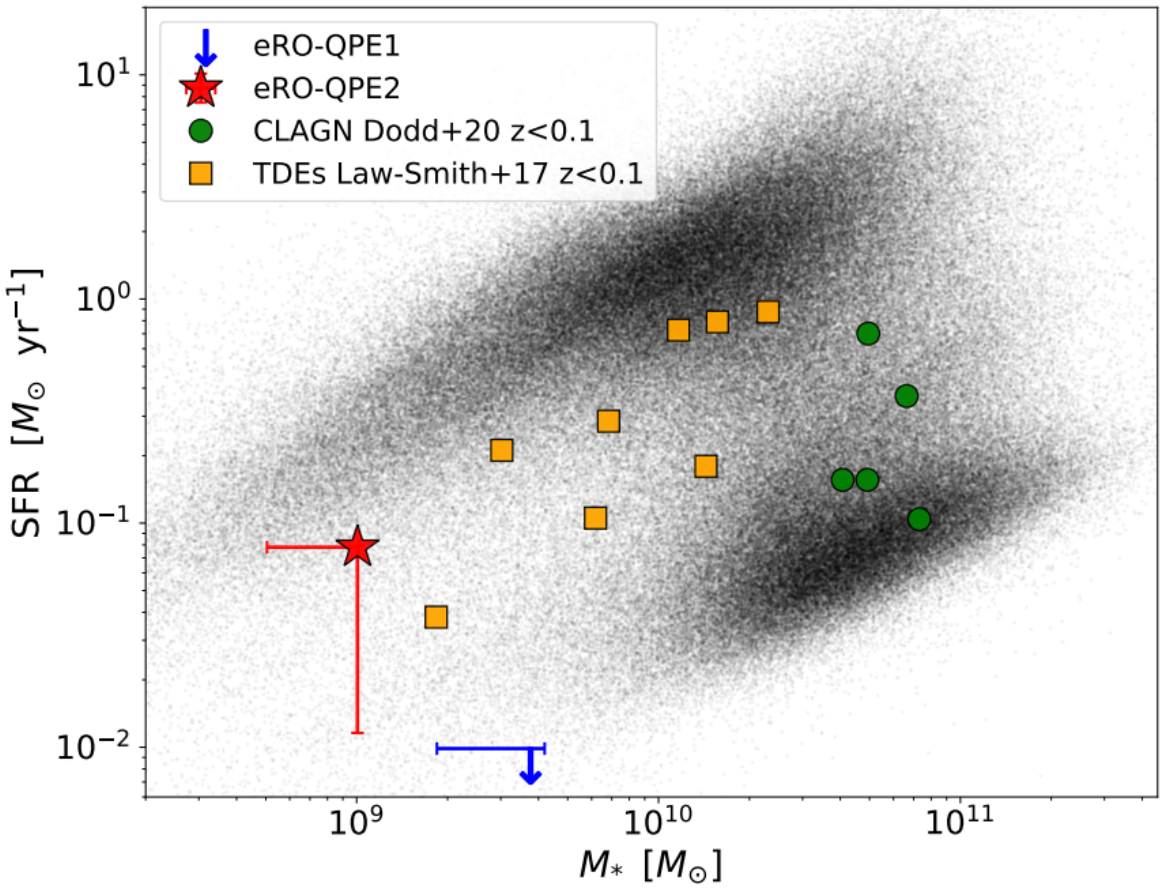

843 **Extended Data Fig. 6 – The properties of QPEs' host galaxies.** Stellar mass M_* and star
844 formation rate (SFR) for eRO-QPE1 (blue) and eRO-QPE2 (red); for eRO-QPE1 SFR is largely
845 unconstrained (see Methods, 'The host galaxies of QPEs'). For a comparison, normal galaxies[67],
846 TDEs[58] and CLAGN[66], all below z<0.1, are also shown.

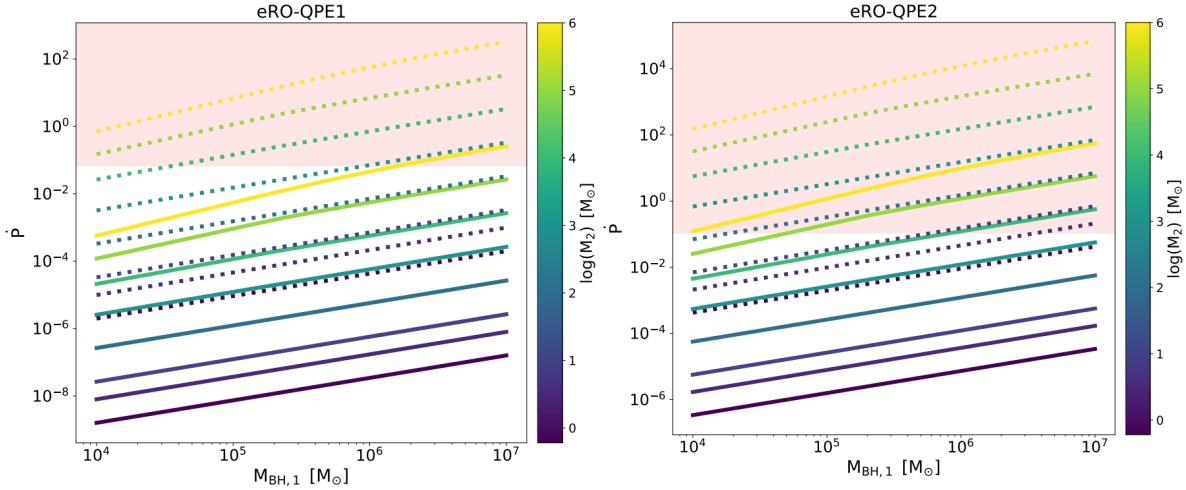

847 **Extended Data Fig. 7 – Constraints on a secondary orbiting body. a**, Allowed parameter space
848 in terms of period derivative and secondary mass M_2 for a range of primary mass $M_{BH,1}$~10^4-10^7
849 $M_\odot$ and zero (solid lines) or high orbit eccentricity (e_O~0.9, dotted lines), in which can reproduce
850 the rest-frame period of eRO-QPE1. We have drawn an approximate threshold at the minimum

period derivative that, if present, we would have measured already within the available observations, corresponding to a period decrease of one QPE cycle over the 15 observed by NICER (Fig. 1d). The excluded region is shaded in red. **b**, same as **a** but for eRO-QPE2 and adopting as tentative minimum $\dot{P}$ a period decrease of one cycle over the 9 observed with XMM-Newton (Fig. 2c).

Extended Data Table 1 - Summary of the observations performed

Source	Instrument	Obs. ID	Start date
eRO-QPE1	eROSITA	-	16 January 2020
	XMM-Newton	0861910201	27 July 2020
	XMM-Newton	0861910301	4 August 2020
	NICER	3201730103	19 August 2020
	SALT	-	24 September 2020
eRO-QPE2	eROSITA	-	23 June 2020
	XMM-Newton	0872390101	6 August 2020
	SALT	-	8 September 2020

Extended Data Table 2 - Summary of spectral fit results for eRO-QPE1

Observation	k_BT [eV]	$F_{0.5\text{-}2.0\ keV}$ [cgs]	F_{disk} [cgs]	$L_{0.5\text{-}2.0\ keV}$ [cgs]
eROSITA low	$\downarrow 160$	$\downarrow 3.4\times10^{-14}$	$\downarrow 2.4\times10^{-13}$	$\downarrow 2.1\times10^{41}$
eROSITA high	180^{195}_{168}	$1.5^{1.7}_{1.4}\times10^{-12}$	$4.2^{4.6}_{3.7}\times10^{-12}$	$0.9^{1.0}_{0.8}\times10^{43}$
XMM quiescence	130^{163}_{103}	$3.8^{5.0}_{2.7}\times10^{-15}$	$1.9^{2.5}_{1.5}\times10^{-14}$	$2.3^{3.1}_{1.7}\times10^{40}$
XMM1 peak	262^{269}_{256}	$3.3^{3.4}_{3.2}\times10^{-12}$	$6.4^{6.6}_{6.2}\times10^{-12}$	$2.0^{2.1}_{1.9}\times10^{43}$
XMM2 peak	148^{156}_{141}	$5.3^{5.6}_{4.9}\times10^{-13}$	$2.0^{2.1}_{1.8}\times10^{-12}$	$3.2^{3.5}_{3.0}\times10^{42}$

The median value and related 16th and 84th percentiles are reported for every quantity; for unconstrained values 1σ upper limits are quoted using the 84th percentile value of the parameter posterior distribution and are denoted with ↓. Reported results are obtained with the model tbabs x diskbb, with Galactic N_H frozen at 2.23×10^{20} cm^{-2}, as reported by the HI4PI Collaboration[48]. Fluxes and luminosities are unabsorbed and rest-frame. The two eROSITA states are shown in Fig.1a, whilst the three XMM-Newton observations in the table correspond to the three spectra in Extended Data Fig. 5a. F_{disk} is computed within 0.001 and 100 keV.

Extended Data Table 3 - Summary of spectral fit results for eRO-QPE2

Observation	$N_H(z)$ [cm^{-2}]	k_BT [eV]	$F_{0.5\text{-}2.0\ keV}$ [cgs]	F_{disk} [cgs]	$L_{0.5\text{-}2.0\ keV}$ [cgs]
eROSITA low	$0.32^{0.38}_{0.28}\times10^{22}$	-	$\downarrow 5.7\times10^{-14}$	$\downarrow 3.4\times10^{-13}$	$\downarrow 4.0\times10^{40}$
eROSITA high	$0.32^{0.37}_{0.28}\times10^{22}$	209^{241}_{185}	$1.5^{1.8}_{1.2}\times10^{-12}$	$3.3^{4.5}_{2.4}\times10^{-12}$	$1.0^{1.3}_{0.8}\times10^{42}$
XMM quiescence	$0.35^{0.40}_{0.30}\times10^{22}$	76^{81}_{70}	$1.7^{2.3}_{1.3}\times10^{-13}$	$8.0^{14.0}_{4.5}\times10^{-13}$	$1.2^{1.6}_{0.9}\times10^{41}$
XMM peak	$0.33^{0.39}_{0.30}\times10^{22}$	222^{249}_{199}	$1.7^{2.1}_{1.5}\times10^{-12}$	$9.1^{14.5}_{4.3}\times10^{-12}$	$1.2^{1.5}_{1.0}\times10^{42}$

Same as Extended Data Table 1, but for eRO-QPE2. Reported results are obtained with the model tbabs x ztbabs x diskbb, with Galactic N_H frozen at 1.66×10^{20} cm^{-2}, as reported by the HI4PI Collaboration[48]; absorption in excess was estimated from 'XMM quiescence' and was allowed to vary within its 10th and 90th percentiles for all the other observations. The two eROSITA states are shown in Fig. 2a and model parameters in the low state are unconstrained; the two XMM-Newton observations in the table correspond to the spectra in Extended Data Fig. 5b.